LIDAR DATA FOR CLASSIFICATION AND SCIENTIFIC MONITORING IN COASTAL AREAS

Alena Schmidt[1], Uwe Soergel[1]

Abstract

In this paper we propose a method for the classification and mapping of habitats in Wadden Sea areas from lidar data. For this task, we derive crucial features from the 3D point cloud based on the geometry and intensity of the backscatter. The characteristics of three different classes (*water*, *mudflat*, *mussel bed*) are learned in a training step of a supervised classification approach. For this purpose, we implement a method capable of modelling context: a Conditional Random Fields framework. From the labeled point cloud 2D objects are generated for the classes *water* and *mussel bed*. Thus, we determine water-land-boundaries as first step towards digital terrain modelling and contribute to the mapping of habitats, two important tasks of coastal monitoring. The results are evaluated on a test site of the German Wadden Sea in the North Sea.

Key words: Lidar, classification, water, Wadden Sea, Conditional Random Fields, digital terrain model

1. Introduction

The Wadden Sea is an intertidal zone located between a section of the coast of north western continental Europe and the Frisian Islands in the southern part of the North Sea. It covers a coastal area of about 10,000 km² and is separated from the North Sea by a barrier island system and ebb-tidal deltas over three quarters of its length. The Wadden Sea consists of tidal mudflats, tidal channels, marshes and other wetlands and exhibits a unique ecosystem which is characterized by a high biodiversity. For these reasons the German and the Dutch parts of the Wadden Sea were inscribed on UNESCO's World Heritage List in 2009. The uniqueness of its habitats is accompanied by a high responsibility towards this area and requires a clear understanding of Wadden Sea's development.

High spatial and temporal variability characterize the Wadden Sea. The ecosystem is significantly influenced by the climate, especially by increasing temperatures. Tidal flows, storms, strong wind, and human activities like dredging or deepening of channels cause changes in the morphology. In order to detect undesired changes at early stages, enabling rapid countermeasures to mitigate or minimize potential harm or hazard, a recurrent monitoring becomes necessary. For the monitoring of coastal areas, basically three techniques are available: terrestrial surveying, echo sounding and remote sensing. Whereas terrestrial surveying is limited by a high cost and time factor and provide only isolated measurements, echo sounding is capable to acquire morphological data with an area-wide coverage. However, due to the limited covered area per day, and the needed sufficient water depth, remote sensing technique becomes a good alternative technique in this context.

In the framework of a German research project called Scientific Monitoring Concepts for the German Bight (WIMO, 2013), new approaches for a sustainable monitoring of coastal areas by remote sensing data are investigated. In particular, the analysis of changes in the morphology and the habitat distribution are of great interest. For these tasks we use three types of remote sensing data: SAR (synthetic aperture radar) data, optical images, and airborne laser scanning data, also called lidar (light detection and ranging). In this paper, we focus on the analysis of lidar data which provide substantial information for two monitoring tasks.

[1]Institute of Photogrammetry and GeoInformation, Leibniz University of Hannover, Nienburger Str. 1, 30167 Hannover, Germany. {alena.schmidt, soergel}@ipi.uni-hannover.de

Firstly, highly accurately digital terrain models (DTMs) of the Wadden Sea are required for a systematic monitoring of morphological changes. They can be used for tasks such hydrographic modelling. Lidar is a standard method for DTM generation in coastal zones (Figure 1) and comes along with two main advantages compared to traditional aerial photogrammetry. On the one hand, the active laser technique works independently from illumination from the sun, which allows mapping also during night-time. On the other hand, the elevation model can be directly inferred from the two-way time-of-flight of the pulse reflected at the ground, whereas stereo techniques rely on matching of corresponding points in two or more image, which requires sufficient texture. In comparison to echo sounding systems, lidar is feasible for large areas and delivers dense and accurate data. However, only the eulittoral zone can be covered by standard laser because the near-infrared laser pulses are not able to penetrate water which remains in some tidal channels even during low tide. Thus, gapless DTM modelling usually requires a combination of height data gathered by echo sounding in the sublittoral zone and airborne lidar systems in the eulittoral zone. Due to the reflection of the near-infrared laser pulses on the water surfaces, the elevation measured by standard lidar represents not the actual terrain level underneath as would be desired. The generation of a DTM thus requires the detection of water surfaces, which leads to a classification of the lidar point cloud into *land* and *water* areas. If such a classification has been carried out, an additional data source, e. g. sonar, could be used to complete the DTM in the water areas. In the future the problem of the combination of two different data sources could be overcome to some extent by laser bathymetry. Such modern devices operate with green laser signal that is capable to penetrate into the water column (e. g. Mandlburger et al., 2011). However, since the accessible depth underneath the water surface depends on turbidity, such technique is better suited for clearer waters compared to Wadden Sea.

Secondly, the classification and mapping of habitats in Wadden Sea areas is an important issue of marine monitoring. We are interested in the contribution of lidar data for the habitat mapping which involves a separation of the class *land* into different subclasses. This has been shown to be possible with spectral information from remote sensing image data (Klonus et al., 2012). Due to the missing of spectral features in the monochromatic lidar signal and the common lack of auxiliary aerial photos to support the classification when the flights are performed during night time, the distinction between habitats based on lidar becomes a difficult task. Given these properties, only habitats characterised by their surface roughness, e.g. *mussel beds*, can be expected to be distinguished. The detection of these areas is of great interest because the cultivation of mussels in the Wadden Sea and the import of exotic species influences the local morphology and change the sediment characteristics (Marencic and de Vlas, 2009). Thus, we differentiate two subclasses of *land*, namely *mudflat* and *mussel bed*.

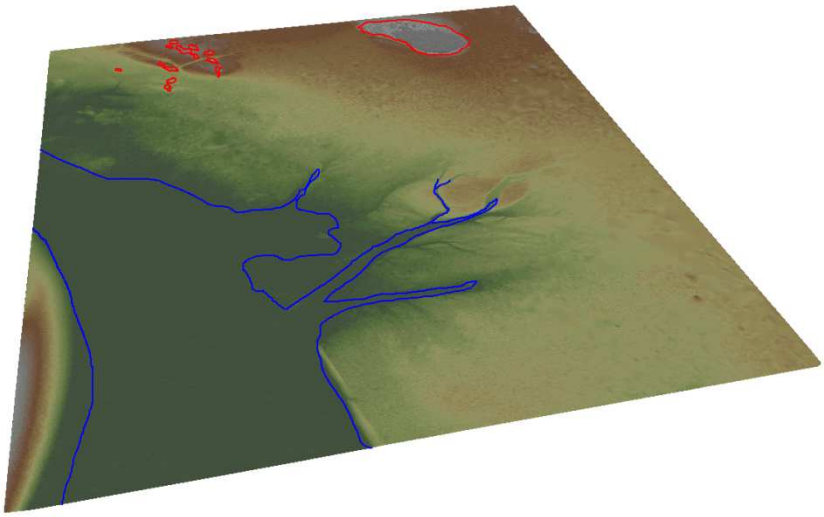

Figure 1. Digital terrain model of a Wadden Sea area generated from lidar data. Water covered tidal channels are outlined in blue, mussel beds in red.

In this paper, we investigate lidar data acquired over Wadden Sea areas in the southeastern part of the North Sea. We focus especially on the classification of the data with the aim to define water-land-boundaries and elaborate the habitat mapping. In this way, we provide a first step towards DTM generation in order to delineate the topography and its dynamics in coastal areas. The second aim of our scientific work is to contribute to a deeper understanding of the habitat composition in coastal areas. Thus, we extend the classification by a third class: *mussel bed*. For the classification we propose a probabilistic approach which incorporates context: Conditional Random Fields (CRF). The labeled point cloud is projected to a 2D label image afterwards and boundaries for water areas and mussel beds are derived.

2. Methodology

Lidar data acquired over Wadden Sea areas are classified in order to generate water-land-boundaries and to detect mussel beds. An overview of the proposed processing chain is given in Figure 2. It can be subdivided into three steps: Firstly, lidar features are derived from the point cloud (section 3). They are introduced in the classification method wherefore we implement an approach based on Conditional Random Fields (section 4). We classify the data based on the row lidar point cloud. After the classification process, each laser point is labeled by one of the tree classes: *land*, *water* or *mussel bed*. Then, object boundaries are calculated based on 2D binary image derived from the labeled point cloud (section 5).

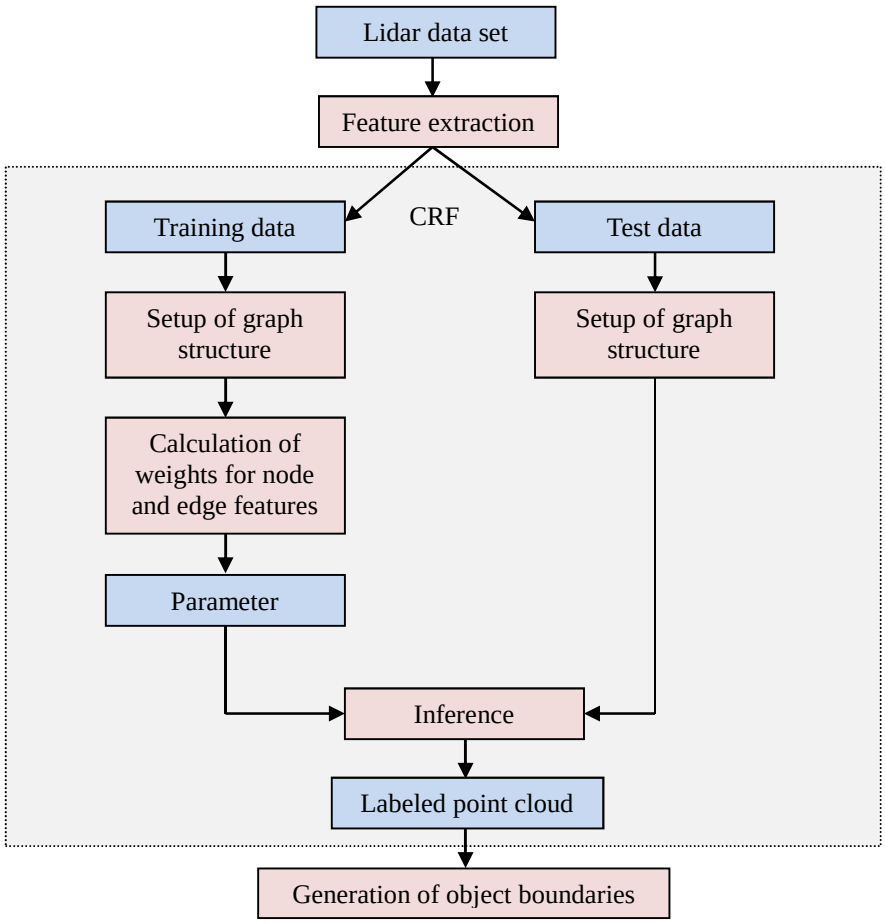

Figure 2. Flowchart of the classification method for lidar data.

3. Lidar features

For each laser pulse, the incoming signal is sampled with very high frequency and stored digitally. From this waveform possible multiple echoes caused by several targets are detected (nevertheless, in case of mudflats we usually deal just with a single echo) by signal processing (e.g., fit of Gaussians to the data). Finally, for each echo the related 3D coordinates and intensity are determined, which is format of the data available for us that covers large parts of the German Wadden Sea.

From these data different features based on the geometry and the intensity are calculated. We adapted some of the features described in Chehata et al. (2009). Because these features are developed for classification tasks in urban areas and deal with the extension of objects (e.g. buildings, vegetation) in all three dimensions, we assume to benefit not from all of them for our special test data. In order to adapt to our data, we expand the model by additional features in our previous work (Schmidt et al., 2012). We calculate 26 classification features for each point. In general, they can be separated into 6 groups: features based on the height (1), the intensity (2), the local distribution of the point cloud (3), the eigenvalues (4), the curvature (5), and the relationship of a point to a local plane (6). Most of them consider the neighbourhood of a point. For this purpose, neighbouring points are searched within a cylinder or sphere of predefined radius centred at the point. We vary the radius r for the neighbourhood search from 1 m to 5 m in steps of 1 m. As a result, the number of features is extended to 124.

In order to minimise the complexity of the approach, we do not use all features for the classification and identify a representative set for our classification task instead. Thus, we analyse the influence of each feature on the classification result by a permutation importance measure which is provided aside classification by a Random Forests approach (Breiman, 2001). For the importance measurement of a feature, its values are randomly permuted. In this way, the absence of this feature can be modelled. Then, the number of correctly classified points before and after permuting the feature is compared. In case of a high difference between both results, the importance of this feature for the classification task is high. The importance can be determined for each class and for the overall classification.

We use the permutation importance measure to identify the most relevant features for our task. For this purpose we consider features whose importances are high for the overall classification and, as the mussel bed detection has proved to be the most challenging task in our previous work (Schmidt et al., 2012), those features which are relevant for the classification of *mussel bed*. Considering both criteria, we choose the following 14 features for our classification:

- absolute height of a point and height variance (r = 4m)
- average height (r = 4m, r = 5m)
- intensity variance (r = 2m, r = 5m)
- point density (r = 1m)
- the lowest eigenvalue (r = 2, r = 3m)
- planarity (r = 4m)
- Gaussian curvature (r = 4m)
- direction (r = 1m) and variance of normal vector (r = 1m, r = 2m).

4. Classification of lidar point cloud

The goal of the classification is to assign an object label to each point of the lidar point cloud. For this purpose, we use a probabilistic supervised classification approach capable of modelling context: Conditional Random Fields (CRF). CRFs are a flexible tool for classification tasks and belong to the group of graphical models. For image labelling, they were introduced in Kumar & Hebert (2006). The classification of point clouds based on CRFs have been developed for instance by Lime & Suter (2009) for the classification of terrestrial laser scanning data. The potential of CRFs for airborne laser scanning data was shown in Shapovalov et al. (2010) (segment-based) and in Niemeyer (2012) (point-wise).

4.1.1. *Conditional Random Fields*

In the CRF framework, a class label C_i from a given set of classes $\mathbb{C}$ is assigned to each lidar point $i \in [1, \dots n]$. The point cloud is classified by finding the optimal label configuration that maximises the posterior probability $P(\mathbf{C}|\mathbf{x})$ of the point labels $\mathbf{C} = [C_1, C_2, \dots, C_n]$ given the observed data $\mathbf{x} = [x_1, x_2, \dots, x_n]$**.** The posterior probability can be modelled by

$$P(\mathbf{C}|\mathbf{x}) = \frac{1}{\mathrm{Z}} exp\big(E(\mathbf{x}, \mathbf{C})\big). \quad (1)$$

In (1) $E(\mathbf{x}, \mathbf{C})$ is an energy term and Z is a normalising constant. The energy term can be expressed by

$$E(\mathbf{x}, \mathbf{C}) \quad = \sum_{i \in S} A(\mathbf{x}, \mathrm{C_i}) + \sum_{i \in S} \sum_{j \in N_i} I\big(\mathbf{x}, \mathrm{C}_i, \mathrm{C}_j\big), \quad (2)$$

where $A(\mathbf{x}, C_i)$ is the *association potential* which indicates the likelihood of a point *i* belonging to a class C_i given the observations $\boldsymbol{x}$ and $I(\mathbf{x}, C_i, C_j)$ is the *interaction potential* which measures how the classes of neighbouring points and data interact. Both terms are described in more detail in the following. The energy term is calculated over the neighbourhood N_i of each point and the dataset *S*.

4.1.2. *Implementation of the graph*

CRFs belong to the group of graphical models. Thus, the data are converted to a graphical model, first. Thereby, the nodes of the graph are represented by the lidar points where adjacent nodes are linked by an edge. A fast access to the nearest neighbours of each lidar point is obtained by indexing the point cloud using a two dimensional k-d tree. Although we deal with three dimensional data, the reduction of one dimension is justified by the appearance of the data. In Wadden Sea there are hardly any objects with a significant extension in height. Nevertheless, the graph of the laser point cloud is an irregular data structure. Each point is linked with its *N* nearest neighbours. A feature vector $\boldsymbol{h}_i(\boldsymbol{x})$ which contains the lidar features described in section 3 is assigned to each node i. In order to consider context, interaction features modelling the relationship of nodes are introduced for each edge linking the node i and j. We calculated the interaction feature vector $\boldsymbol{\mu}_{ij}(\boldsymbol{x})$ as the absolute difference of feature vectors $\boldsymbol{h}_i(\boldsymbol{x})$ and $\boldsymbol{h}_j(\boldsymbol{x})$ of neighbouring nodes i and j. In case of a similar feature characteristic of neighbouring points the entries in the interaction vector $\boldsymbol{\mu}_{ij}(\boldsymbol{x})$ are low which imply that the points belong to the same class. In contrast they show high values for dissimilar features which suggest the presence to different classes.

4.1.3. *Training*

The method is a supervised classification approach. Thus, classification parameters have to be learnt in a training step. Following equation (2) the posterior probability consists of the *association* and the *interaction potential*. For the *association potential* any local discriminative classifier resulting in a probability $P(C_i|\boldsymbol{h}_i(\boldsymbol{x}))$ can be applied. Closely related to Kumar & Hebert (2006) we use a generalized linear model for that purpose. Then, $A(\boldsymbol{x}, \mathrm{C}_i)$ can be expressed as

$$A(\boldsymbol{x}, C_i = l) = \boldsymbol{w}_l{}^T \boldsymbol{h}_i(\boldsymbol{x}). \quad (3)$$

In (5) vector $\boldsymbol{w}_l$ contains the weights of node features and is determined by a training step. Such a vector is

defined for each class l. The probability that a pair of adjacent nodes i and j has the labels C_i and C_j is described by the *interaction potential* $I(\boldsymbol{x}, C_i, C_j)$. Analogous to the *association potential* $A(\boldsymbol{x}, C_i)$ it can be modelled being proportional to $\log P\left(C_i, C_j|\boldsymbol{\mu}_{\mathrm{ij}}(\mathbf{x})\right)$, obtained again by a generalized linear model:

$$I\left(\boldsymbol{x}, C_i = l, C_j = k\right) = \boldsymbol{v}_{l,k}^T \boldsymbol{\mu}_{ij}(\boldsymbol{x}), \tag{4}$$

where $\boldsymbol{v}_{l,k}$ is the weight vector of the interaction features. Such a vector $\boldsymbol{v}_{l,k}$ exists for each combination of classes (l, k). In the training process the optimal values for the weight vectors are derived from training data. The use of exact probabilistic methods for this is computationally intractable. Thus, they are replaced by approximate solutions. Here, we applied the gradient descent optimisation method of L-BFGS (limited memory Broyden–Fletcher–Goldfarb–Shanno) (Liu & Nocedal, 1989) for the minimisation of the objective function $f = -\log(P(\theta|\boldsymbol{x}, \boldsymbol{C})$, where θ contains the weight vectors $\boldsymbol{w}_l$ and $\boldsymbol{v}_{l,k}$.

4.1.4. *Inference and labelling of the point cloud*

The optimal label configuration is determined in an inference step. Thereby, $P(\boldsymbol{C}|\boldsymbol{x})$ is maximised for given parameters based on loopy belief propagation (Frey & MacKey, 1998), a standard iterative message passing algorithm for graphs with cycles. The result is one probability value per class for each data point. The optimal label configuration based on maximising $P(\mathrm{C}|\boldsymbol{x})$ is provided via maximum a posterior (MAP) probability estimate.

5. Object generation

In order to define land-water-boundaries and to determine the covering of mussel beds, an object generation is performed afterwards. Thus, the labeled 3D point cloud is projected to a 2D label image. For both classes, *water* and *mussel bed*, a binary image is derived where nonzero pixels belong to an object and zero pixels to the background. Then, the exterior boundaries of the objects and possible holes inside these objects are determined. In a post-processing step small objects are removed and small holes are closed by a morphological opening.

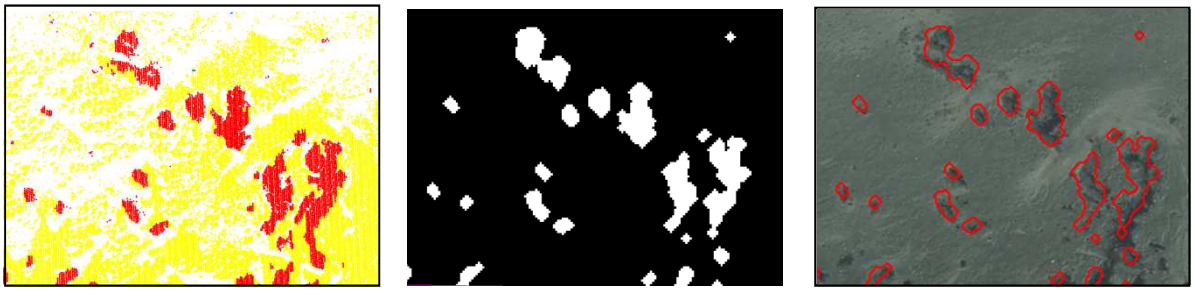

Figure 3. The labeled point cloud (left) is projected to a binary image (middle) of which mussel bed objects are generated and compared with an orthoimage (right).

6. Results and Discussion

6.1 *Dataset*

We evaluate our approach on a lidar dataset of the German Wadden Sea. It is located in the south of the East Frisian Island Norderney in the North Sea and contains one big tidal channel from north to south which is followed by tidal currents. Although the data were acquired during low tide, water still remains there, especially in the bigger tideways whereas the smaller ones partly dry to muddy channel. In the western part of the tidal channel several mussel beds cover the test area. The lidar data acquisition was carried out with the Trimble Harrier 56 in spring of 2010. The size of the test area is 750 m x 400 m where approximately 1 million points are recorded. Whereas the point density is mostly high, the dataset shows the typical effect of lidar data acquired over water surfaces (and even areas with a small water film): the laser pulses are specular reflected. Dependent on the incidence angle the backscatter cannot be recorded by the sensor which leads to gaps in the data set.

6.2 *Classification results*

We classify the point cloud by the CRF approach described in section 4 and distinguish between three classes: *water*, *mudflat*, and *mussel bed*. During the graph generation each point is linked to its two nearest neighbours by an edge. For each point and respectively for each edge we use the 14 features described in section 3 and a quadratic feature space mapping. For the training step we generate a manually labeled reference point cloud including all classes and class interactions. We use approximately 10 % of the points from the dataset for training. For the qualitative evaluation we compute the *completeness* and *correctness* rates (Heipke et al. 1997).

The classification results are shown in Figure 4 and Table 1. It can be seen that most of the points on water surfaces are detected which is evidenced by a high completeness rate of 95.1 %. Some misclassifications occur near to the mudflat boundaries where local height differences are low. Another issue is that the dataset consists of data from four different flight strips. Due to different acquisition times of each flight strip, the water level differs slightly caused by tidal effects. Thus, the characteristics of water surfaces vary in the overlap of two strips which leads to some misclassification in these parts. The problem could be overcome by classifying each flight strip separately.

As shown in table 1, the completeness and correctness rate of *mussel bed* are lower in comparison to the class *water*. Misclassifications are caused by similar feature characteristics of the point cloud near to tidal

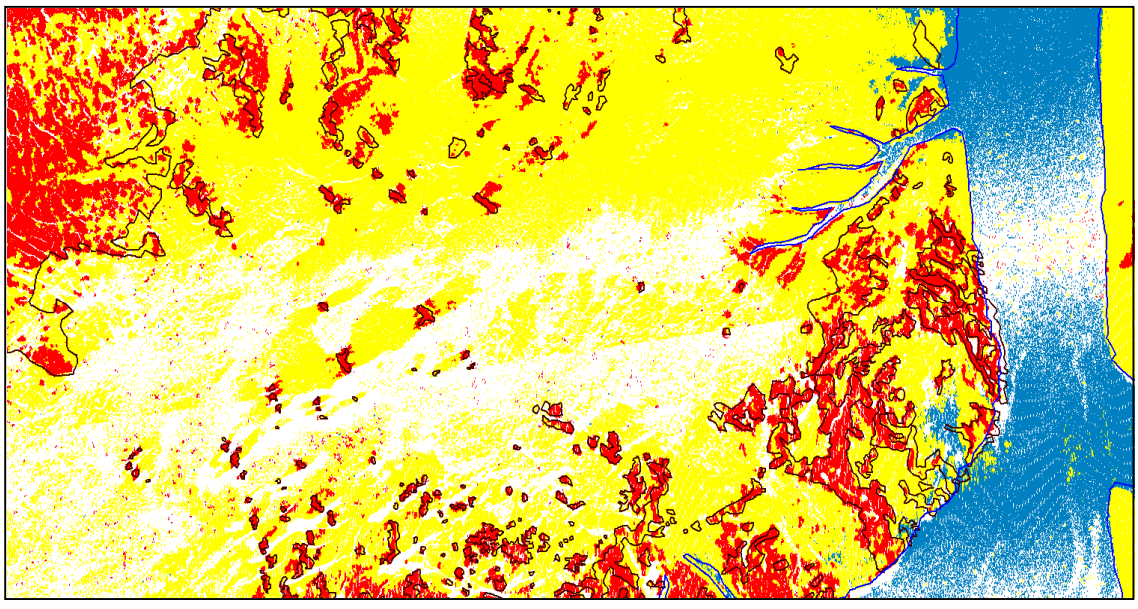

Figure 4. Labeled point cloud of the test site in the German Wadden Sea for the classes *water* (blue), *mussel bed* (red) and *mudflat* (yellow). Areas with no return are coloured in white. The references of water and mussel beds are outlined in blue and black.

channels where larger local height differences and deviations of neighbouring points from a local plane occur, too. In regard to different sizes of the mussel beds, their appearance in the laser data varies in some parts and, thus, we do not benefit from the chosen radii in the feature calculation for all points reflected on mussel beds. Moreover, some rough mudflat structures are incorrectly depicted as *mussel bed.*

class	*mudflat*	*water*	*mussel bed*
correctness	89.3 %	90.2 %	60.1 %
completeness	86.1 %	95.1 %	65.8 %

Table 1. Correctness and Completeness rate for the three classes.

6.3 *Object generation*

In order to define water-land-boundaries and boundaries of mussel beds respectively, objects are generated in a pre-processing step. The lidar points assigned to *water* or *mussel bed* are projected to a label image. For the elimination of small objects and to close holes inside, we use a morphological opening. Thus, the number of single misclassified points, especially single *mudflat* points which are depicted as *mussel bed,* can be eliminated, whereas on water surfaces holes in the classification result are closed. The resulting boundaries of *water* and *mussel bed* are shown in Figure 5. Due to not correctly classified water points in the overlapping part of two flight strips, the water surface of the big tidal channel is separated into two objects. Moreover, small holes still remain in the water surfaces which could be eliminated by stronger smoothing. However, the water-land-boundaries can be used as important input value concerning the terrain modelling. While the digital terrain model generated from the lidar point cloud ensure a high accuracy beyond the water surfaces, an additional data source, e.g. sonar, could be used to complete the DTM in these parts. The detected mussel bed boundaries can provide the basis for a habitat mapping of the Wadden Sea.

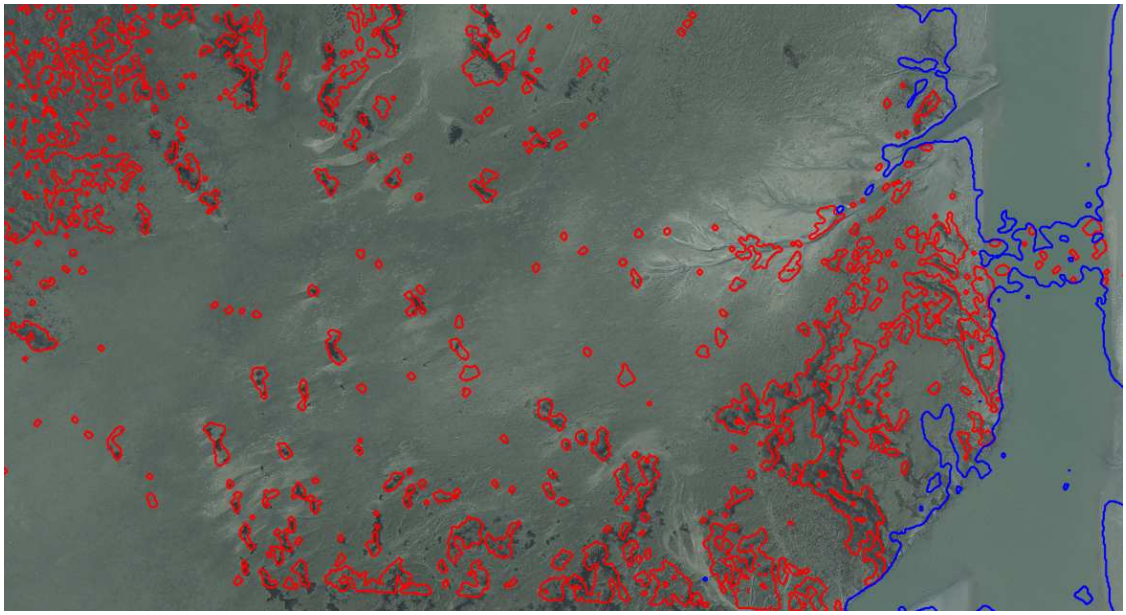

Figure 5. Orthoimage and generated objects of the classes *water* (blue) and *mussel bed* (red).

7. Conclusion and Outlook

In this paper we presented a classification approach for lidar data in Wadden Sea areas. In regard to a habitat mapping and the generating of DTMs, the lidar point cloud is assigned to the classes *mudflat*, *water* and *mussel bed*. We show suitable lidar features for this task. They are derived from the geometry and the intensity of the three-dimensional point cloud. For the classification, we implemented a supervised approach based on CRF. In this way, context can be integrated in the classification. The evaluation on a test site of the German Wadden Sea showed good results for the detection of *water* in lidar data. Only in the overlapping part of different flight strips some misclassifications are caused by slightly differing height levels due to tidal effects. Based on local height differences, curvatures and deviations from a local plane, it is also possible to detect *mussel beds* in lidar data. However, they are classified in a lower rate of correctness and completeness. We observed two reasons for this: First, mussel beds are confused with rough mudflat parts. Secondly, their size various significantly. From the labeled point cloud 2D *water* and *mussel bed* objects are generated afterwards. By using morphological operations on the label image, the number of small misclassified objects can be reduced. The boundaries of the *water* and *mussel bed* objects provide an important input value concerning terrain modelling respectively the habitat mapping of the Wadden Sea.

In the future we intend to integrate some texture features in the classification process. We also plan to combine our results with those obtained from optical and SAR images in order to establish a reliable concept for the marine monitoring.

References

Breiman, L., 2001. Random forests. *Machine Learning* 45 (1): 5–32.

Chehata, N., Guo, L., Mallet, C., 2009. Airborne lidar feature selection for urban classification using random forests. *The International Archives of the Photogrammetry, Remote Sensing and Spatial Information Sciences*, Vol. XXXVIII, Part3/W8, Paris, France: 207–212.

Heipke, C., Mayer, H., Wiedemann, C. & Jamet, O., 1997: Evaluation of automatic road extraction. *International Archives of Photogrammetry and Remote Sensing* **32** (3-4,W2): 151–160.

Klonus, S., Ehlers, M., Schmidt, A., Soergel, U., Adolph, W. and Farke, H., 2012. Change detection in wadden sea areas using RapidEye data, *Proceedings of the 32nd Earsel Symposium 2012*, Mykonos Island: 18-25

Kumar, S. and Hebert, M., 2006. Discriminative Random Fields. *International Journal of Computer Vision*, 68(2): 179 –201.

Lim, E.H. and Suter, D., 2009. 3d Terrestrial Lidar Classifications with Super-Voxels and Multi-Scale Conditional Random Fields. *Computer-Aided Design*, 41(10): 701–710.

Mandlburger, G., Pfennigbauer, M., Steinbacher, M. and Pfeifer, N., 2011: Airborne Hydrographic LiDAR Mapping - Potential of a new technique for capturing shallow water bodiesh, *Modelling and Simulation Society of Australia and New Zealand*", (2011): 2416 - 2422.

Marencic, H. and de Vlas, J. (Eds), 2009. Wadden Sea - Quality Status Report 2009. Wadden Sea Ecosystem 25. Trilat eral Monitoring and Assessment Group, Common Wadden Sea Secretariat, Wilhelmshaven, Germany.

Niemeyer, J., Rottensteiner, F., and Soergel, U., 2012. Conditional random fields for lidar point cloud classification in complex urban areas. *ISPRS Annals of the Photogrammetry, Remote Sensing and Spatial Information Sciences*, I-3: 263-268.

Schmidt, A., Rottensteiner, F., and Soergel, U., 2012. Classification of airborne laser scanning data in wadden sea areas using conditional random fields. *International Archives of the Photogrammetry, Remote Sensing and Spatial Information Sciences XXIX-B3:* 161-166.

Shapovalov, R., Velizhev, A. and Barinova, O., 2010. Non-associative Markov Networks for 3d Point Cloud Classification. *International Archives of the Photogrammetry, Remote Sensing and Spatial Information Sciences*, 38/Part A: 103–108.

WIMO, 2013. Wissenschaftliche Monitoringkonzepte für die Deutsche Bucht (Scientific Monitoring Concepts for the German Bight), http://wimo-nordsee.de (March 4, 2013)